

Simulation of Acidification of the Golgi-Apparatus

2.1.2007

Ulf W. Liebal *

Physiology of the Golgi-apparatus

The Golgi-apparatus is physiologically distinguishable as a narrow succesion of about six membrane enclosed compartments to build a recognizable stack phenotype.

The Golgi apparatus fullfills its role in the cellular symphony as the main protein and lipid sorting and processing agency. Proteins travel via vesicles from the endoplasmatic reticulum (ER) to the cis Golgi cisternae if they possess the appropriate signal sequence that mark them as Golgi destined proteins. Sorting by the Golgi characterizes the default pathway of protein secretion for essential proteins such as neurotransmitter, hormones and digestive enzymes. Likewise, integral membrane proteins are transported to the surface of the cell via the Golgi mediated trafficking and also the maintenance of the protein constitution of Lysosomes and Endosomes is established by Golgi sorting. Once the proteins arrive at the cis Golgi face they are further chemically processed for example by glycosylation, phosphorylation, sulfation among others and mature proteins are proteolytically cleaved from precursor proteins in the Golgi. [12]

As it is true for the cytosol also in the Golgi apparatus the proceeding reactions are highly sensible to changes of the proton concentration, i.e. the pH. Most reactions depend upon proton transitions and the distribution of protonated or deprotonated residues in the active site of enzymes. Slight pH changes as of 0.5 can fundamentally change the reaction parameters and disturb the cellular system. One strategie that controls the accurate delivery of biosynthetic cargos in the Golgi to their destinations is the interaction of the cargos with their respective receptor molecules. The interaction of cargo and receptor itself is modulated by the state of protonation of the participating proteins such that protein interactions loosens or strengthens when certain pH values are reached. The previous arguments reveal the stringent dependence of a functional Golgi apparatus to a fine tuned pH regulation. This strong dependence can be assessed with respect to phenotypes that arouse due to pertubations. It is reported that a forced equilibration of Golgi and Cytosolic pH impairs posttranslational modifications, the cargo molecules are misdirected and the integrity of the organelle itself is compromised. The influenza virus exploits the pH regulation of the Golgi for the final virus assembly. Influenca inserts its own proton channel into the Golgi membranes and invokes an alkalanization of the Lumen towards cytoplasmic pH. This retards the overall protein traffic and facilitates the assemby of the virus.

*contact: ulfliebal@web.de

[15] Furthermore results by Rivinoja et al. show that certain types of tumor cells have a significant alkalinized pH in the Golgi Lumen compared to healthy cells [16].

Several mechanisms take part in the regulation of the pH of the Golgi lumen but most attention received the proton influx via V-ATPases and the proton leakage, whereas the effects of membrane potential, counterion permeability or metabolic activity are thought to play negligible roles [15].

V-ATPase activity: The H^+ pumping vacuolar-type ATPase (V-ATPase) is located in the membranes of archaebacteria, some eubacteria and in endomembranes of all eukaryotic cells [19]. It is structurally similar to the F-ATPase that mitochondria use for generation of ATP. The V-ATPase pumps protons with the expense of ATP to build a proton motive force (pmf) i.e. to acidify compartments in the case of the Golgi. The maximum pH gradient attainable by the V-ATPase when neglecting the membrane potential can be calculated by laws of thermodynamics and amounts to $\Delta pH \sim 4.6$ at physiological conditions [4]. Since the pH in the Golgi is more alkaline compared to the lowest thermodynamically attainable pH the V-ATPases are pumping at a high rate and other factors remove protons at the steady state [18]. The activity of the V-ATPase is approximately linear with respect to the luminal pH, therefore allosteric regulation is not likely to play a prominent role in pH regulation [15, 18].

Proton leakage, i.e. the passive or facilitated diffusion, that is driven by the concentration gradients between the Cytoplasm and the Golgi Lumen, is one process by which protons can be withdrawn from the Lumen. It is assumed that the steady state pH values of different organelles is set by the magnitude of the proton leakage of the respective organelar membrane [15, 18, 21]. Support for this notion is given by experiments that show that the pH recovery following an acid load is the fastest for organelles that have a higher luminal steady state pH indicating a higher proton permeability [21]. The nature of the leakage pathway is still obscure in detail but it was found that it shares a similarity with the H^+ -specific conductance found in the plasma membrane of several cell types in that both are inhibited by addition of Zn^{2+} [18].

Buffering capacity (β) describes another process by which protons could be removed from the Lumen. The term describes the binding of H^+ to weak bases to form the corresponding weak acid. The buffering capacity of a solution is determined by the pKa's of all occurring weak bases and the amount varies usually for different pH values in the cell [3]. However, measurements of the buffering capacity in organelles with different steady state pH revealed similar values implying that the buffering capacity and pH had reached already a steady state [22].

Membrane potential and counterion permeability: The V-ATPase activity is electrogenic and builds a positive membrane potential that will grow until the proton motive force (pmf), i.e. the energy that is needed to pump a proton, is larger than the available energy given by hydrolysis of ATP. The pmf is composed of the proton concentration gradient and the gradient of the electric potential, that is the membrane potential. The impeding effect of the membrane potential can be reduced by the movement of counterions over the membrane that dissipate charge differences. Favourite candidates as counterions are chloride that follows the proton movement and potassium that moves opposite to protons. If the membrane potential would limit the acidification of the Lumen it would imply that the movement of counterions is slower than the proton intrusion rate. The dependence of acidification on counterion movement was tested by addition of valinomycin, an ionophore that allows virtually unlimited exchange of potassium through the membrane, to cells and measuring the acidification. By that no change in the steady state level of luminal pH could be detected therefore indicating that the electrical potential across the Golgi membrane is insignificant [15, 18, 21]. Investigations in the effect of chloride were performed by incubation of cells in Cl^- free solution, but no difference in luminal pH to the Cl^- containing control could be measured in these experiments [21].

Other channels are present in the membrane of the Golgi apparatus that could effect pH regulation. Isoforms of the Na^+/K^+ -ATPase have been found to reside in the Golgi membrane and to alkalin-

ize the Lumen when overexpressed [13]. However, in experiments in the presence of amiloride, an inhibitor of several isoforms of the Na^+/K^+ -ATPase, the resting pH of the Golgi was not affected and a sudden increase of the cytosolic Na^+ concentration did not affect Golgi pH [18].

The anion exchangers $AE1$, $AE2$ and $AE3$ mediate the Na^+ -independent Cl^-/HCO_3^- exchange and contribute to the regulation of intracellular pH, cell volume, tonicity and intracellular chloride in metazoan cells [20]. Their importance for luminal pH regulation is not determined in full detail yet, but findings suggest that the isoform $AE2$ is genuinely located in the Golgi membrane [8, 7]. There are several other Cl^- transporters in the membrane and experiments with Cl^- -free solutions did not affect luminal steady state pH but bicarbonate imported to the lumen could act as a weak base and increase the buffering capacity to halt further acidification.

The Golgi anion channel (GOLAC) is a channel that mediates chloride exchange that may allow the observed dissipation of the membrane potential by providing high permeability to Cl^- . Likewise the channel could act as a gateway for inorganic phosphate that is generated extensively due to glycosylation or sulfation of proteins and lipids in the Lumen [14]. As a channel GOLAC is a mean of facilitated diffusion and does not need to be modelled explicitly, instead an adapted permeability for affected ions and the usage of the Goldman-Hodgkin-Katz equation (6) is appropriate.

Investigation into pH regulation

The pH has a profound impact on cellular functions and attempts of simulations for the sake of a thorough understanding were made first with whole cell models [23, 11]. Only recently models have been constructed that describe the pH regulation of eukaryotic organelles. Rybak and co-workers built a theoretical model of the acidification of Endosomes from a thermodynamic viewpoint on the basis of the Nernst equation and examined the achievable steady state pH values when different ions were allowed to migrate actively in the system and assuming a constant buffering capacity [17]. With the drawback that no passive or facilitated diffusion is included the authors come to the conclusion that the main pH regulating factors in Endosomes are 1) the concentration of negative fixed charges in the interior of the organelle, 2) the buffering capacity (β) and/or 3) Na^+/K^+ -ATPase activity. Moreover the membrane potential is of prominent importance for endosome acidification in contrast to the assumed Golgi acidification.

A kinetic model of the pH regulation of the Golgi based on ordinary differential equations was constructed by Grabe & Oster that allows the simulation of time resolved equilibration processes [3]. In their model the authors simulate the activity of the V-ATPase and account for the movement of sodium, potassium and chloride over the membrane. The chloride movement is only diffusion controlled whereas sodium and potassium are additionally exchanged by Na^+/K^+ -ATPase. The membrane potential was computed as the excess charge within the lumen and the difference in proton concentration of Cytoplasm and Lumen. Additionally, the buffering capacity was included either as a constant parameter or as depending on the pH with a best fit function of experimental data. Neglected are influences to the pH by biochemical reactions, biochemical differences of cis, medial and trans Golgi and the volume surface area and the number of pumps does not change during the course of a simulation. In the model the resting pH is the most sensitive to the H^+ permeability, i.e. the leakage rate, as well as to the number of V-ATPases. In contrast the acidification time line is most sensitive to the buffering capacity, the luminal volume and the Golgi surface area. By fitting the simulation to experimental data the Golgi proton permeability was estimated as $\sim 10^{-5} cm/s$. In the case of endosome acidification which can be limited by the activity of the Na^+/K^+ -ATPase the model suggests that either the endosomal membrane contains a voltage-gated Cl^- -channel, which is in accordance with results by Rybak mentioned earlier or that the initial internal potassium concentration

is far greater than typical external values and no Cl^- conductance. [3]

Theoretical composition of pH regulation

Membrane potential

In two separated compartments a membrane potential may exist caused by different electric potentials on both sides of a membrane which in turn is caused by unequal ionic charge distributions:

$$V_m = \phi_i - \phi_e \quad (1)$$

with the electrical potentials ϕ in the internal (i) and external (e) compartment. In the electric circuit model the membrane is regarded as a capacitor that separates charges and the membrane potential can be expressed as

$$V_m = \frac{Q}{C_m S} \quad (2)$$

where C_m represents the capacitance, S the surface area and Q the separated charges that can be calculated via:

$$Q = FVol_i \left(\sum [cations]_i - \sum [anions]_i \right) - FVol_e \left(\sum [cations]_e - \sum [anions]_e \right) \quad (3)$$

containing cation and anion concentrations on both sides, the volume (Vol) and Faraday's constant (F).

For the case of simulation of the Golgi pH one can often assume that the ionic concentrations in the cytoplasm behave like situated in an infinite bath, that is their concentration will not change due to in- or efflux of the Golgi. Furthermore, given the demand of electroneutrality of the cell the overall cation and anion concentrations in the cytoplasm have to be equal, therefore the righthand side in the difference of eq. (3) can be ignored. A detailed analysis of the membrane potential was made by [2].

Surface charges have implications on the concentration distributions of species in proximity of the membrane such that cations will be attracted by negative surface charges raising their concentrations. This effect can be modelled with a Boltzmann factor [3]:

$$[X_{i,0}] = [X_i] \exp \left(-\frac{zF\Delta\phi_{i,0}}{RT} \right) \quad (4)$$

relating the phenomenological potential difference $\phi_{i,0}$ between the bulk volume and the membrane facing the volume, z as the valence of the ion and F , R and T with their common meanings to the surface concentration $X_{i,0}$. Lipid bilayer are asymmetric giving the cytoplasmic leaflet in frog nerve cells a negative surface potential of -30 mV. The effect of surface potentials induced concentration differences on the activity of pumps is disputed, since these have a relatively large distance from the bilayer. [3]

Modelling diffusion – Goldman-Hodgkin-Katz Equation

In general diffusion is modelled by the Nernst-Planck equation that relates diffusion caused by concentration gradients and the electric field:

$$J = -D \left(\nabla[X] - [X]z \frac{F}{RT} \nabla\phi \right) \quad (5)$$

where D denotes the diffusion coefficient, $[X]$ designates the concentration of the species, ϕ as the electric potential. With the assumption that diffusion takes place only over one dimension and that the electric field over the membrane is linear the flux J can be derived as the constant field approximation/Goldman-Hodgkin-Katz (GHK) equation:

$$J = Pz \frac{FV_m}{RT} \frac{[X]_i - [X]_e \exp\left(-\frac{zV_m}{RT}\right)}{1 - \exp\left(-\frac{zV_m}{RT}\right)} \quad (6)$$

with P representing the permeability of the specie ($= \frac{D}{L}$, diffusion coefficient divided by membrane thickness L), V_m describing the membrane potential and $[X]$ with subscripts i , e designates the internal, external species concentration, respectively. For a detailed discussion see [9, 6].

The GHK equation is generally used to described the flux of ions over a membrane for passive and facilitated diffusion. In the case of facilitated diffusion only the permeability of the species is assumed to increase. Effects of facilitated diffusion like saturation of transport are not modelled with the GHK equation.

V-ATPase activity

Grabe et al. constructed a detailed mechanochemical model of the function of the V-ATPase based on structural and biochemical considerations [4]. The V-ATPase consists of a stationary part, the stator and a rotationally moving part, the rotator. Cytoplasmic H^+ is in equilibrium with binding sites of the rotator but the rotator cannot pass a hydrophobic strip in the stator until the negatively charged binding site is protonated. However, once neutralized by protonation, the torque from V1 subunit drives the site across the barrier into the stator output channel. In the output channel the proton binding site interacts with a positively charged site chain that reduces the pK_a value to the proton and thereby releasing it to the luminal site. The unprotonated negatively charged proton binding site then enters the polar strip and subsequently faces the cytosolic volume again to complete the cycle. The functioning of the pump is very detailed and ingeniously modelled by Grabe et al. and the resources of their calcuations are available as matlab files. The output of these files generate a matrix whose components solve for the proton flux for a pH ($pH: 4 - 7.6$, step: 0.2) and membrane potential range($V_m: -80 - 260$ mV, step: 20 mV). The entries of the matrix can therefore be used as approximation for a fast calculation of the proton flux at given pH and V_m . [4] A comparison for the calculation of acidification following the explicit model of Grabe et al. with a simulation using the coarse grained matrix is shown in Fig. 1.

In particular they described the state of the V-ATPase as a function of the angular position θ of the proton binding sites via:

$$\frac{ds}{dt} = K(\theta) s \quad (7)$$

with $K(\theta)$ as a transition matrix between chemical states of the proton binding site s , i.e. the dissociation and association of protons, of which 16 distinguishable states exist with four binding sites and two realizations ($2^4 = 16$). The motion of the rotor of the V-ATPase is obtained by equating the viscous drag on the motor with the forces that act on the rotor:

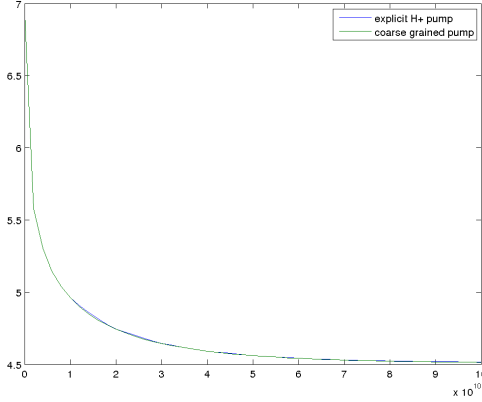


Figure 1: The acidification of a compartment by action of the V-ATPase is shown for the explicit model of Grabe et. al (blue line) as well as using coarse grained values, see text for details. Differences in the acidification curve are only minor so that the usage of the coarse grained matrix is justified.

$$\zeta \frac{d\theta}{dt} = \tau_Q(\theta, s) + \tau_{\Delta\phi}(\theta, s) + \tau_{\Delta\epsilon}(\theta, s) - \tau_D(\theta) + \tau_B(t) \quad (8)$$

whereby $\zeta \frac{d\theta}{dt}$ reflects the frictional drag, $\tau_Q(\theta, s)$ represents the rotor-stator charge interaction, $\tau_{\Delta\phi}(\theta, s)$ designates the membrane potential, $\tau_{\Delta\epsilon}(\theta, s)$ models the dielectric barrier, $\tau_D(\theta)$ is the driving torque from the V₁ subunit and $\tau_B(t)$ is the Brownian torque. The motion is solved with a Fokker-Planck equation that calculates the probability density of finding the rotor at angular position θ at time t .

A simplified model of the V-ATPase activity was developed by Luo et al. and used in their macrophage cell model for pH and volume regulation [10, 11]. Although, or probably because, the model is simpler some of the used derivations require a deeper understanding of the physics and mathematics of the system in question. Finally, they arrive at a fairly straight forward equation for the V-ATPase proton flux. The author of these lines was not able to implement this "simple" model into the pH simulation, and instead used the resources given by Grabe et al..

Na⁺/K⁺-ATPase

The Na^+/K^+ -ATPase exchanges three Na⁺ from the Cytoplasm for two K⁺ from the Golgi lumen and is therefore electrogenic.

Heyse et al. constructed an exhaustive model of the activity of the Na^+/K^+ -ATPase composed of 14 differential equations [5], that was also used and adopted in the Golgi pH model by Grabe & Oster [3]. However, Luo et al. used an approximation to the sodium-potassium flux in their macrophage cell model that is simpler in this case [11]:

$$v_{Na,K} = V_{max} \frac{V_m + V_a}{V_m + V_b} \left(\frac{[K_e^+]}{[K_e^+] + K_{mK}} \right)^2 \left(\frac{[Na_i^+]}{[Na_i^+] + K_{mNa}} \right)^3 \quad (9)$$

where $v_{Na,K}$ describes the speed of the sodium, potassium exchange, V_{max} describes the maximal speed of the transport, $V_{a,b}$ are constants and $K_{m(K,Na)}$ designates the equilibrium binding constant

for potassium and sodium respectively. Eventually, for reasons of consistency and accuracy, the detailed model of Grabe & Oster should be applied for the Na^+/K^+ -ATPase in the model.

The AE2 activity

The detailed mechanism of the mode of action of the anion exchanger family is currently not known, a model has therefore to be constructed on an empirical basis most likely based on the assumption of Michaelis-Menten kinetics comparable to the Na^+/K^+ -ATPase of Luo et al..

Buffering capacity & Donnan potential

According to the Brønsted theory acids and bases are capable of donating and accepting protons:



with B being a weak base. An equilibrium constant can be formulated as follows:

$$K = \frac{[B^{(n)}][H^+]}{[HB^{(n+1)}]} \quad (11)$$

or alternatively in form of the Henderson–Hasselbalch equation:

$$pH = pK + \lg \frac{[B^{(n)}]}{[HB^{(n+1)}]} \quad (12)$$

The weak acid and weak base of formula (10) forms a buffer pair that is capable of reversibly binding or releasing a proton, and thereby acting as a buffer. The buffering capacity is defined as the amount of strong base – or the negative of the amount of strong acid – that alters the pH by a certain amount:

$$\beta = \frac{OH_{added}^-}{\Delta pH} = -\frac{H_{added}^+}{\Delta pH} \quad (13)$$

The buffering effects can be subdivided into buffering in open and closed systems. In the latter the amount of total buffer remains constant throughout the time, for example an inorganic phosphate solution, whereas in the former an external source and sink for the buffer species may exist, for example a NH_4^+/NH_3 buffer system of a cell in an infinite bath. (see [1] for a picturesque description)

A model of the pH regulation of the macrophage, including buffering effects of the NH_4^+/NH_3 buffer pair was built by Luo et al. [11]. In their model the authors follow the change of the total buffer concentration as $B_{tot} = B^{(n)} + HB^{(n+1)}$ in (10) with $B^{(n)}$ as NH_3 and $HB^{(n+1)}$ as NH_4^+ by the sum of the GHK-equation (6) governed flux for NH_4^+ and simple concentration dependent diffusion for NH_3 . Furthermore, it is assumed that the membrane diffusion processes take considerably more time than the reactions of the buffer pair with protons such that the equilibrium for the buffer is always reached and that therefore species concentrations can be obtained via the equilibrium formulation (11). The attributions of the buffering system to the proton concentration is then calculated as the amount of NH_4^+ that is formed in equilibrium and subsequently diffuses out of the cell (thereby removing a proton), and the change of protons in response to a new equilibrium state due to NH_3 efflux. (see [11] and therein equation 25 for the detailed formula):

$$\frac{dH^+}{dt} = f \left(\underbrace{-\frac{K_{NH_3}}{K_{NH_3} + [H_i^+]} J_{NH_4^+}}_{\text{flux of equilibrium } NH_4^+} + \underbrace{\frac{[H_i^+]}{K_{NH_3} + [H_i^+]} J_{NH_3}}_{\substack{H^+ \text{ change due to} \\ NH_3 \text{ flux}}} \right) \quad (14)$$

The effect of the buffering capacity on the change of the proton concentration can be described as follows [23]:

$$\frac{dH^+}{dt} = \frac{2.3[H^+]}{\beta} \{ (\# \text{ protons added per unit time}) - (\# \text{ protons taken out per unit time}) \} \quad (15)$$

The buffering capacity does not effect the steady state pH, but the dynamic response of the pH depends strongly on the buffering capacity [3, 23]. The buffering capacity of carbondioxide, β_{CO_2} , is $2.3[HCO_3^-]$ if CO_2 is kept constant and the level of CO_3^{2-} is negligible compared to that of HCO_3^- [23].

The negative charge of the immobile matrix proteins of the Golgi has to be balanced by mobile counter ions which will then generate a Donnan potential. The immobile Donnan particles have to be included in the calculation for the membrane potential.

Other transporters located in the Golgi membrane

As mentioned earlier an anion channel was detected in the Golgi membrane which is capable of enhancing the diffusion of chloride and inorganic phosphate of Cytoplasm and Lumen [14]. One may assume that the GOLAC (Golgi anion channel) is abundant and is not limiting for the diffusion process. In that case an explicit model of the channel is not necessary, instead an adapted permeability coefficient is acceptable. Likewise other chloride transport mechanisms are present in the membrane like the AE2. However, if chloride transport is significant it may reach saturation of GOLAC for a certain concentration. Then it is appropriate to model chloride diffusion additionally by a Michaelis-Menten type process.

Na^+/H^+ exchanger (NHE) have been detected to reside in the Golgi membrane and it was observed that the NHE promotes proton efflux from the Golgi [13]. However other studies suggest a minor role of NHE mediated ion transfer, since the absence of Na^+ caused no change in steady state pH [18]. A complete model of the Golgi acidification will have to implement NHE activity and judge its importance.

Golgi volume change and osmotic pressure

The geometrical structure has an influence on the acidification since the charge of ions is computed following eq. (3), wherein the concentration is multiplied with the volume. For the calculation of the membrane potential, eq. (2), the surface area is in the denominator, so that effectively the volume-surface relation determines the membrane potential. Likewise, the GHK equation (6) describes the specie flux per time and unit area. To arrive at the total number of particles that are transported into the Lumen the GHK flux has to be multiplied with the surface over which diffusion takes place and

has to be multiplied by the volume in order to get from species concentration to the number of specie molecules.

A sensitivity analysis of the Golgi pH model by Grabe & Oster revealed that organelle volume and surface area have profound impact on the kinetics of the acidification but none on the steady state pH [3].

Osmosis describes the flux of water (J_W) to balance differences in ion concentrations:

$$J_W = P_W S \left(\sum_k \frac{\psi_{k,i}}{a_k} [X_{k,i}] - \psi_e \right) \quad (16)$$

with P_W , S as water permeability, surface area, respectively, $\psi_{k,i}$ as the osmotic coefficient of specie k , a_k as the solute activity, subscripts i,e designate internal, external localization and ψ_e is the osmolarity of the external solution or the cytoplasm. Any in- or efflux of species into the lumen will affect the osmolarity of the solution, water will flow according to eq. (16) and the volume will change. Luo et al. modelled this volume change for ion concentration variations in the macrophage as [11]:

$$\frac{d(Vol_i [X_e]^{tot})}{dt} = Vol_i \sum_k \frac{d[X_{k,i}]}{dt} \quad (17)$$

correlating the internal volume Vol_i with the total extracellular ion concentrations $[X_e]^{tot} = \sum_k [X_{k,e}]$ with $[X_{k,e}]$ as a concentration for the external ion X_k , and $[X_{i,k}]$ as the internal concentration of ion X_k .

A basic model example

The following set of differential equations could simulate the acidification of the Golgi lumen including the membrane potential (18), diffusion following GHK (6), V-ATPase activity (7, 8):

$$V_m = \frac{F Vol}{C_m S} ([H^+]_i - [H^+]_e + [Na]_i + [K]_i - [Cl]_i - [B]) \quad (18)$$

$$\frac{dH^+}{dt} = \left(\underbrace{\text{V-ATPase pump}}_{\substack{\text{V-ATPase activity} \\ \text{described in eqs. 7, 8}}} \cdot \underbrace{\varrho_{\text{V-ATPase}}}_{\substack{\text{density of} \\ \text{V-ATPase pumps}}} \right. \underbrace{- \frac{P_{H^+} F V_m}{RT} \frac{[H^+]_i - [H^+]_e \exp\left(-\frac{V_m}{RT}\right)}{1 - \exp\left(-\frac{V_m}{RT}\right)} N_a}_{\substack{\text{GHK-diffusion, eq. 6}}} \left. Vol S \right) \quad (19)$$

$$\frac{dNa^+}{dt} = - \frac{P_{Na^+} F V_m}{RT} \frac{[Na^+]_i - [Na^+]_e \exp\left(-\frac{V_m}{RT}\right)}{1 - \exp\left(-\frac{V_m}{RT}\right)} N_a Vol S \quad (20a)$$

$$- 3 \cdot \underbrace{\text{Na}^+/\text{K}^+ \text{ATPase}}_{\substack{\text{active Na}^+ \text{ efflux} \\ \text{following eq. 9}}} \cdot const. \quad (20b)$$

$$\frac{dK^+}{dt} = -\frac{P_{K^+} F V_m}{RT} \frac{[K^+]_i - [K^+]_e \exp\left(-\frac{V_m}{RT}\right)}{1 - \exp\left(-\frac{V_m}{RT}\right)} N_a \text{ Vol } S \quad (21a)$$

$$+ 2 \cdot \underbrace{\text{Na}^+/\text{K}^+ \text{ATPase}}_{\substack{\text{active K}^+ \text{ influx} \\ \text{following eq. 9}}} \cdot \text{const.} \quad (21b)$$

$$\frac{dCl^-}{dt} = \frac{P_{Cl^-} F V_m}{RT} \frac{[Cl^-]_i - [Cl^-]_e \exp\left(\frac{V_m}{RT}\right)}{1 - \exp\left(\frac{V_m}{RT}\right)} N_a \text{ Vol } S \quad (22)$$

The V-ATPase pump provides the activity for one single pump so the result has to be multiplied with the amount of active pumps ($\varrho_{\text{V-ATPase}} \cdot S$ in eq. 19). Estimation of the density of V-ATPases range from ~ 500 to 2000 pumps per μm^2 and allow therefore only a crude estimation given additional uncertainties with the Golgi surface area S [4].

The flux of sodium and potassium can move by either only diffusional fluxes described in eqs. 20a, 21a, or as in eqs. 20b, 21b additionally by active pumping of the Na^+/K^+ -ATPase for sodium, potassium respectively. The occurring parameter const. in eqs. 20b, 21b is purely arbitrarily and serves to raise the pump activity to values where it can significantly influence ion flow with respect to diffusion. To fulfill this role const. takes a dimension of about 10^8 , the parameter could be interpreted as the amount of pumps in the Golgi membrane.

Ion concentrations can be adapted for surface potentials following eq. 4 with $\phi_{e,0}$, the surface charge in the cytoplasm of 50 mV [3].

Observations in the current model

Figure 2 illustrates the equilibration of the Lumenal pH either only driven by diffusion, such that the luminal pH will equal the cytoplasmic pH (a), or with additional consideration of V-ATPase activity which acidifies the Lumen by about 0.5 pH units (b). In the one ion case of figure 2 the membrane potential is an important parameter for the equilibrium condition. As can be seen in eq. 19 in the case when only diffusion takes place (figure 2(a)) the change of the proton concentration becomes zero only if the membrane potential becomes zero. If the V-ATPase pump is active then equilibrium is reached when the diffusional efflux equals the active proton influx. For that to happen the proton difference for the compartments will reach a certain value and this proton difference will give rise to a nonzero membrane potential (figure 2(b)). The membrane potential is very low compared to physiological conditions due to the minuscule concentrations of the protons of $10^{-7} \frac{\text{mol}}{\text{l}}$ that allow according to eq. 18 only membrane potentials in the order of 10^{-4} V . The wavy pattern that occurs in the beginning of the equilibration process is introduced by the numerical solving procedure of the Matlab ODE solver.

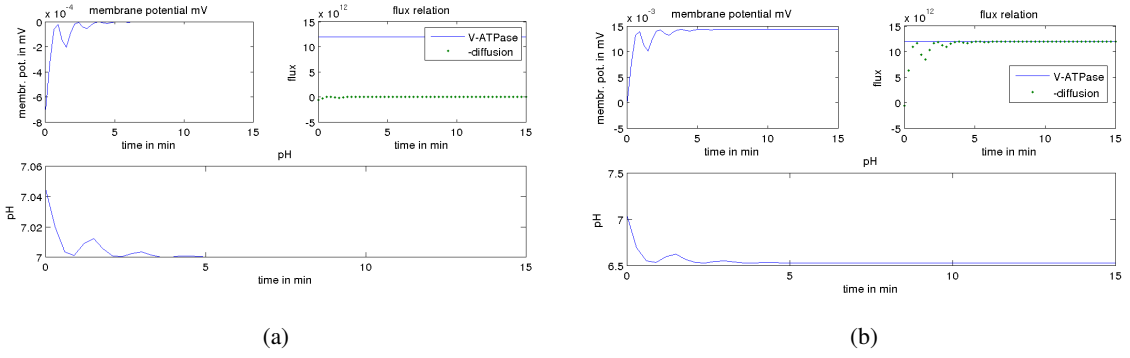


Figure 2: Simulation of Lumen pH when (a) no V-ATPase is active such that only diffusion equilibrates pH between Lumen and Cytoplasm, (b) a V-ATPase pumps protons into the Lumen. For the simulation protons are considered to be the only moving ion species.

Figure 3 depicts a simulation in which beside protons another positively charged ion, here designated as K^+ , is allowed to move passively over the membrane. Again, as the V-ATPase is active, the Lumen gets acidified by proton influx which generates a positive membrane potential. This positive membrane potential drives potassium out of the Lumen to reset the membrane potential to zero. Since the potassium concentrations is much higher than the proton concentration, different potassium values in figure 3 are not visible. Again equilibrium is reached when proton efflux is adapted to the influx, as seen in the subfigure flux relations. The undershoot of the pH in figure 3 is due to the numerical solving procedure.

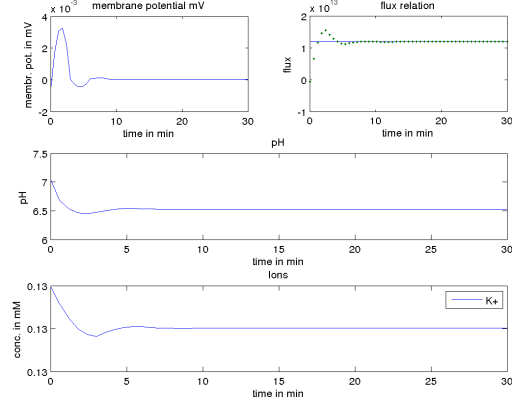


Figure 3: Simulation of Lumen acidification if beside protons another positively charged ion is present. The other ion, here called K^+ , only moves via diffusion. Protons are pumped in addition into the Lumen by V-ATPase activity.

An active Na^+/K^+ -ATPase, one that is more effective compared to diffusion, rises the membrane potential in the model significantly by pumping three Na^+ inside the lumen and only removing two K^+ . The build up of the positive membrane potential opposes further acidification of the Lumen. However, once the Na^+/K^+ -ATPase reaches a steady state with constant Na^+ and K^+ concentrations in the compartments acidification can proceed to a pH similar to a situation without Na^+/K^+ -ATPase, see figure 4. Since the Michaelis-Menten binding constant (K_M) for K^+ is much smaller

in the model of Luo et al. than the binding constant for Na^+ the export of K^+ is very sensible of the internal potassium concentration and at equilibrium and will always be smaller than the external sodium concentration (given the infinite bath assumption in the cytoplasm). Since at physiological conditions the K^+ concentration is high, only slightly lower than in cytoplasm but in the simulation of figure 4(b) the potassium concentration drops sharply, care is needed with evaluation of the results. In contrast figure 4(a) shows the evolution of the ionic concentrations mainly governed by diffusion, showing understandably that concentrations of Lumen and Cytoplasm approximate each other.

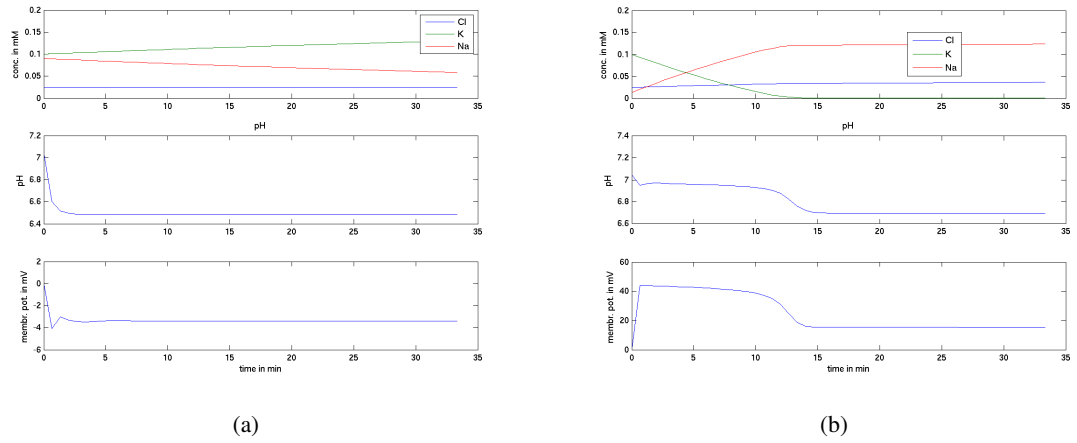


Figure 4: Simulation of Lumen pH, membrane potential and ion concentrations of Cl^- , Na^+ and K^+ when protons are pumped via a V-ATPase following activity of Grabe & Oster [3] and diffusion governed movements of the other ions (a), or additionally to the V-ATPase a Na^+/K^+ -ATPase following the model of Luo et al. [11] is actively exchanging Na^+ and K^+ (b).

Figure 5 includes surface charges on the cytoplasmic side in the simulation modelled according eq. 4 with a potential difference ϕ on the cytoplasmic side of +50 mV as used by Grabe & Oster [3]. Figure 5(a) shows a simulation if surface charges are excluded with the result that the pH drops constantly to around 6.5 and a membrane potential of little less than -4 mV. However, including surface charges the membrane potential rises until around +45 mV and accordingly the resting pH is higher at around 6.7. Additionally the movements of ions via diffusion proceed faster such that the adaption of Cl^- , Na^+ and K^+ concentrations adapt earlier to their steady state values.

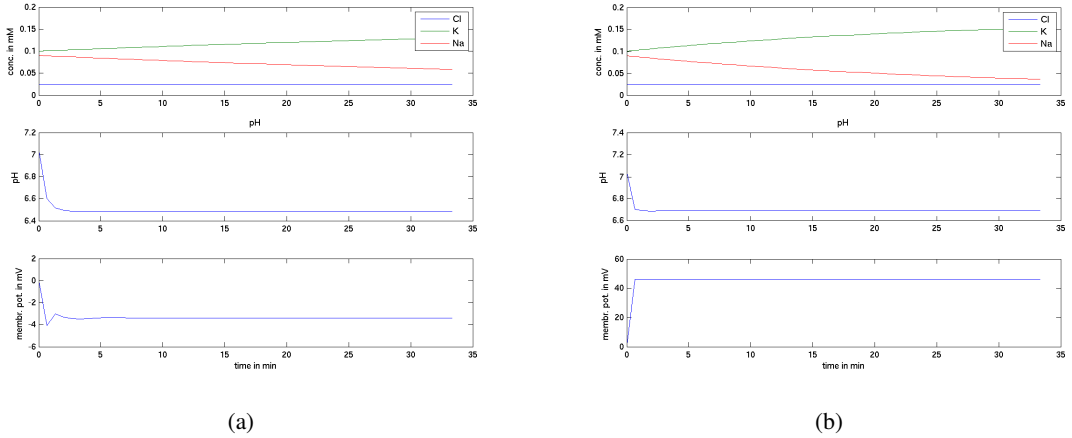


Figure 5: Simulation of luminal pH, membrane potential and ionic concentrations for a compartment with proton influx via V-ATPases modelled according to Grabe & Oster [3] without (a) or including (b) surface potentials modelled after eq. 4, with no luminal surface charge but a cytoplasmic potential difference of +50 mV.

Summary

The Golgi apparatus fulfills a vital role in the cell functioning by processing and distribution of lipids and proteins. A thorough knowledge of the working mechanisms of the Golgi apparatus is desirable since some of the most important illnesses like influenza and cancer are connected with the Golgi. A computer simulation based on a theoretical model can test our degree of knowledge about the system and can essentially support the explanation of experimental observation as well as the prediction of new unobserved properties of the system under investigation. A veritable model of the Golgi pH regulation can eventually form the basis of a pharmaco-kinetic approach in which information about the system can be used to study the mode of action of therapeutically useful drugs in the Golgi to ease pathogenic phenotypes. With use of pharmaco-kinetic methods the search for new biological active compounds can be dramatically accelerated and targeted.

The new acidification model of the Golgi that is to be built will include previous modelling attempts by Grabe & Oster but will have to go beyond this successful previous attempts to also include additional factors. The most important of these factors is the activity of the AE2 and the effect of the imported or exported weak base HCO_3^- on buffering capacity and acidification.

References

- [1] W. Boron. Regulation of intracellular pH, 2004.
- [2] L. Endresen, K. Hall, J. Høye, J. Myrheim. A theory for the membrane potential of living cells. *European Biophysics Journal*, 29(2):90–103, 2000.
- [3] M. Grabe, G. Oster. Regulation of Organelle Acidity. *The Journal of General Physiology*, 117(4):329–344, 2001.
- [4] M. Grabe, H. Wang, G. Oster. The Mechanochemistry of V-ATPase Proton Pumps. *Biophysical Journal*, 78(6):2798–2813, 2000.

- [5] S. Heyse. Partial reactions of the Na, K-ATPase: determination of rate constants. *The Journal of General Physiology*, 104(2):197–240, 1994.
- [6] B. Hille. *Ionic channels of excitable membranes*. Sinauer Associates Sunderland, Mass, 1992.
- [7] K. Holappa, S. Kellokumpu. Targeting of the AE2 anion exchanger to the Golgi apparatus is cell type-dependent and correlates with the expression of Ank (195), a Golgi membrane skeletal protein. *FEBS Lett*, 546(2-3):257–64, 2003.
- [8] K. Holappa, M. Suokas, P. Soininen, S. Kellokumpu. Identification of the Full-length AE2 (AE2a) Isoform as the Golgi-associated Anion Exchanger in Fibroblasts. *Journal of Histochemistry and Cytochemistry*, 49:259–270, 2001.
- [9] J. Keener, S. Wiggins, L. Sirovich, L. Kadanoff, J. Sneyd. *Mathematical Physiology*. Springer, 2001.
- [10] C. Luo, J. Clark Jr, T. Heming, A. Bidani. A simplified model for V-ATPase H⁺ extrusion. *IEEE Trans Nanobioscience*, 3(4):257–64, 2004.
- [11] C. Luo, J. Clark Jr, T. Heming, A. Bidani. A macrophage cell model for pH and volume regulation. *Journal of Theoretical Biology*, 238(2):449–463, 2006.
- [12] S. Mogelsvang, K. Howell. Global approaches to study Golgi function. *Curr Opin Cell Biol*, 2006.
- [13] N. Nakamura, S. Tanaka, Y. Teko, K. Mitsui, H. Kanazawa. Four Na/H Exchanger Isoforms Are Distributed to Golgi and Post-Golgi Compartments and Are Involved in Organelle pH Regulation. *Journal of Biological Chemistry*, 280(2):1561–1572, 2005.
- [14] M. Nordeen, S. Jones, K. Howell, J. Caldwell. GOLAC: An Endogenous Anion Channel of the Golgi Complex. *Biophysical Journal*, 78(6):2918–2928, 2000.
- [15] P. Paroutis, N. Touret, S. Grinstein. The pH of the Secretory Pathway: Measurement, Determinants, and Regulation. 19(4):207–215, 2004.
- [16] A. Rivinoja, N. Kokkonen, I. Kellokumpu, S. Kellokumpu. Elevated Golgi pH in breast and colorectal cancer cells correlates with the expression of oncofetal carbohydrate T-antigen. *Journal of Cellular Physiology*, 208:167–174, 2006.
- [17] S. Rybak, F. Lanni, R. Murphy. Theoretical considerations on the role of membrane potential in the regulation of endosomal pH. *Biophysical Journal*, 73(2):674–687, 1997.
- [18] F. Schapiro, S. Grinstein. Determinants of the pH of the Golgi Complex. *Journal of Biological Chemistry*, 275(28):21025–21032, 2000.
- [19] V. Schoonderwoert, G. Martens. Proton Pumping in the Secretory Pathway. *Journal of Membrane Biology*, 182(3):159–169, 2001.
- [20] A. Stewart, N. Kerr, M. Chernova, S. Alper, R. Vaughan-Jones. Acute pH-dependent Regulation of AE2-mediated Anion Exchange Involves Discrete Local Surfaces of the NH₂-terminal Cytoplasmic Domain. *Journal of Biological Chemistry*, 279(50):52664–52676, 2004.

- [21] M. Wu, M. Grabe, S. Adams, R. Tsien, H. Moore, T. Machen. Mechanisms of pH Regulation in the Regulated Secretory Pathway. *Journal of Biological Chemistry*, 276(35):33027–33035, 2001.
- [22] M. Wu, J. Llopis, S. Adams, J. McCaffery, M. Kulomaa, T. Machen, H. Moore, R. Tsien. Organelle pH studies using targeted avidin and fluorescein-biotin. *Chem. Biol.*, 7:197–209, 2000.
- [23] P. Wu, N. Ray, M. Shuler. A computer model for intracellular pH regulation in Chinese hamster ovary cells. *Biotechnology Progress*, 9(4):374–384, 1993.